Steel Structures Research Update

Continuity Plate Design for Special and Intermediate Moment Frames

JUDY LIU

INTRODUCTION

Recent advances in continuity plate design for special and intermediate moment frames are highlighted. The featured research includes a comprehensive experimental and computational study by Dr. Chia-Ming Uang and Dr. Mathew Reynolds. Chia-Ming Uang is a professor of structural engineering at the University of California, San Diego (UCSD). Dr. Uang is an internationally recognized leader in structural steel research and standards development, with an emphasis in seismic-resistant design. Dr. Uang's numerous accolades include AISC's Special Achievement Award in 2007, the T.R. Higgins Lectureship Award in 2015, and this year, AISC's Lifetime Achievement Award. Dr. Reynolds completed this research as his doctoral work at UCSD under Dr. Uang's guidance and is now working as a bridge engineer for Kiewit in Burnaby, British Columbia, Canada.

The full-scale test program and computational parametric study supported the use of fillet welds to replace expensive complete-joint-penetration (CJP) groove welds adjoining the continuity plate to column flanges. A simplified weld design procedure, as well as local buckling design criteria, are being developed for potential inclusion in the next edition of the AISC *Seismic Provisions for Structural Steel Buildings* (AISC, 2016a). The motivation for the study, the proposed design methodology, and selected experimental and computational results are presented.

BACKGROUND AND MOTIVATION

There are some possibly conservative design and detailing requirements for prequalified connections in special and intermediate moment frames. The conservative provisions include welding and geometric requirements for continuity plates and come with cost implications. Continuity plates, shown in Figure 1, stiffen the column for the concentrated forces and deformations from the beam flanges.

Continuity plates are required when the column has insufficient strength for the concentrated forces or does not satisfy prescriptive geometric limits. Applicable limit states include local flange bending (LFB), web local yielding (WLY), and web local crippling (WLC) of the column. The available strength of the column is calculated following the AISC *Specification* (AISC, 2016b). AISC *Seismic Provisions* Equation E3-8 also requires continuity plates when the column flange thickness is less than the beam flange width divided by 6 (AISC, 2016a). In this study, the minimum unstiffened column flange thickness requirement has been named the "Lehigh criterion," acknowledging the source.

The continuity plates and their welds have additional, sometimes expensive, requirements. The continuity plate must be at least 50% as thick as the adjacent beam flange thickness for exterior (one-sided) connections. For interior (two-sided) connections, the continuity plate thickness must be at least 75% that of the thicker adjacent beam flange. The weld between the continuity plate and the column flange is required to be a CJP groove weld. Compared to fillet welds, the CJP groove welds are more expensive due to the fabrication of the beveled plates, fabrication and installation of backing bars, potential for additional weld volume, and more stringent inspection requirements. From the fabrication point of view, it would be highly desirable if fillet welds were permitted.

Additional motivation for this investigation came from a pilot study by Mashayekh and Uang (2018). The pilot study included tests of two exterior reduced beam section (RBS) connections with fillet-welded continuity plates. The study was focused on use of an elastic, flexibility design method for the continuity plates originally developed by Tran et al. (2013). But continuity plates of one specimen were intentionally undersized to permit yielding. The satisfactory performance observed for the connection with continuity plate yielding inspired, in part, the test program for the featured study.

RESEARCH OBJECTIVES AND PROPOSED DESIGN METHODOLOGY

The overarching research goal was to develop and validate a more efficient, plastic design methodology for continuity plates and use rationally designed fillet welds to attach continuity and doubler plates. The focus for this article is on

Judy Liu, PhD, Research Editor of the AISC *Engineering Journal*, Professor, Oregon State University, School of Civil and Construction Engineering, Corvallis, Ore. Email: judy.liu@oregonstate.edu

the continuity plates and their welds. For the objective of improving the economy of continuity plates, the proposed methods for sizing the plate and fillet welds were verified experimentally and numerically. Requirements dictating the use of continuity plates—for example, the Lehigh criterion—were also studied. Full-scale testing provided supporting evidence in two phases: the first phase investigated reduced beam section (RBS) one-sided connections, and the second phase examined welded unreinforced flange–welded web (WUF-W) two-sided connections. Detailed finite element analysis was used to parametrically study and verify the proposed design methodology.

The proposed plastic methodology for the continuity plates has basis in the current provisions of the AISC *Specification* (AISC, 2016b). The demand on the continuity plate considers the beam flange force and the column strength associated with FLB, WLY, and WLC. The continuity plate is analyzed for in-plane axial and shear forces, and its ultimate strength is verified with a plastic interaction equation (Dowswell, 2015). A capacity design philosophy was used to develop a simple rule for sizing the fillet welds that join the continuity plates and the column flanges. The strength of a transverse, double-sided fillet weld of size w was compared to the nominal yield strength of the plate. For an A572 Gr. 50 continuity plate of thickness t_{cp} and a fillet weld made with a matched weld electrode, the rule is $w = (¾)t_{cp}$.

EXPERIMENTAL TESTING

The test setup and loading were designed to impose deformations corresponding to increasing levels of interstory drift on moment frame subassemblies. Figure 2 shows an interior moment connection specimen in a horizontal test setup. The cruciform test subassembly represented a portion of a prototype moment frame, extending half the bay width to either side for each beam and half the story height above and below the beam-column joint. The ends of the test beams and columns were at assumed inflection points in the prototype moment frame. The loading corbels, hinge, and clevis supports in the test frame were designed to provide the appropriate boundary conditions. Lateral beam bracing was also provided in accordance with the AISC *Seismic Provisions* requirements for highly ductile members. For the interior moment connection tests, two 500-kip hydraulic actuators were used in displacement control for the cyclic loading protocol prescribed in the AISC *Seismic Provisions* (AISC, 2016a). The imposed displacements were applied equal and opposite on either side of the connection. The exterior moment connections were tested using a similar setup but in an upright position and with a single 220-kip hydraulic actuator. Additional test setup, loading, and instrumentation information can be found in Reynolds (2020).

Test Specimens

The test program included 10 full-scale specimens. These moment connection specimens were designed to evaluate the efficacy of economized continuity plate and doubler plate weld details (Reynolds, 2020). Six one-sided, or exterior, RBS connections (C series) were tested in phase 1. Four two-sided, or interior, WUF-W connections (W series) were tested in phase 2. The beams and columns were all ASTM A992 W-shape sections. Beam, column, and connection

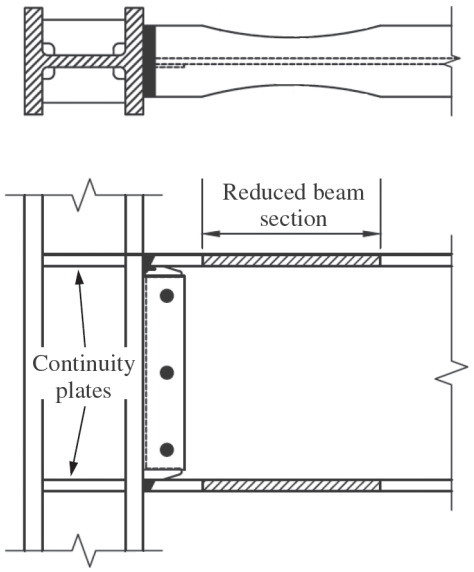

Fig. 1. Reduced beam section (RBS) moment connection with continuity plates.

design and detailing satisfied the AISC *Seismic Provisions* (AISC, 2016a) and the AISC *Prequalified Connections for Special and Intermediate Steel Moment Frames for Seismic Applications* (AISC, 2020) requirements except as noted. The continuity and doubler plates were fabricated from ASTM A572 Gr. 50 steel. Simulated field welding was used for the beam top and bottom flange CJP groove welds and beam web CJP groove weld. The continuity plate and doubler plate weld electrodes satisfied notch-toughness requirements for demand critical welds specified in AWS D1.8 (AWS, 2016).

The phase 1 RBS specimens were used to explore the proposed design methodology for the continuity plates and their welds. FLB and WLY were considered in the plastic design methodology. It was noted that WLC rarely governs in special moment frames (SMFs) using rolled wide-flange shapes. A number of specimens were used to test the current requirement that an unstiffened column flange is at least as thick as the adjacent beam flange width divided by 6 (AISC, 2016a), the Lehigh criterion.

The phase 2 WUF-W specimens were used to investigate the validity of the proposed methodology for continuity plates with higher demands associated with a two-sided WUF-W connection. High panel-zone shear demands dictated the use of doubler plates in all specimens; three of the four specimens used extended doubler plates that protrude beyond the continuity plate at the beam flange elevation. The final specimen used a doubler plate cut flush with the inside face of the continuity plates.

Three test specimens, two RBS and one WUF-W, will be described here. Specimens C5, C6, and W2 were all designed to investigate the validity of using the plastic distribution to estimate the required strength of the continuity plate. Some test specimen details are provided in the following sections. Additional details for these specimens and the rest of the test program can be found in Reynolds and Uang (2019).

Reduced Beam Section (RBS) Specimen C5

The panel zone, continuity plate thickness, and weld size were important parameters for specimen C5 [Figure 3(a)]. The reduced section in the W36×150 beam had dimensions as shown in Figure 3(b). The W14×211 column was designed to have a weak panel zone, with a demand-to-capacity ratio of 1.18. The intent was to exacerbate column kinking. The continuity plates were sized using the plastic design method, with a deliberately high width-to-thickness ratio of 16.0. The continuity plates did not satisfy the AISC *Seismic Provisions* requirement of a thickness at least half that of the beam flange thickness for exterior connections. Local buckling, together with column kinking, was expected to impose significant inelastic demands on the continuity plates and the welds. Meanwhile, the continuity plate welds to the column flanges were sized using the proposed $w = (¾)t_{cp}$ rule.

Reduced Beam Section (RBS) Specimen C6

Continuity plate thickness was also an important parameter for specimen C6. The reduced section in the W30×116 beam had dimensions as shown in Figure 4. The continuity plates were sized using the plastic design method. The plates did satisfy the AISC *Seismic Provisions* requirement of a thickness at least half that of the beam flange thickness for exterior connections. Meanwhile, the continuity plate welds to the W24×176 column flanges were conservatively sized as $w = t_{cp}$. The intent of the oversized fillet welds was to avoid possible premature failure and to allow for investigation into the effects of galvanization with a companion specimen C6-G.

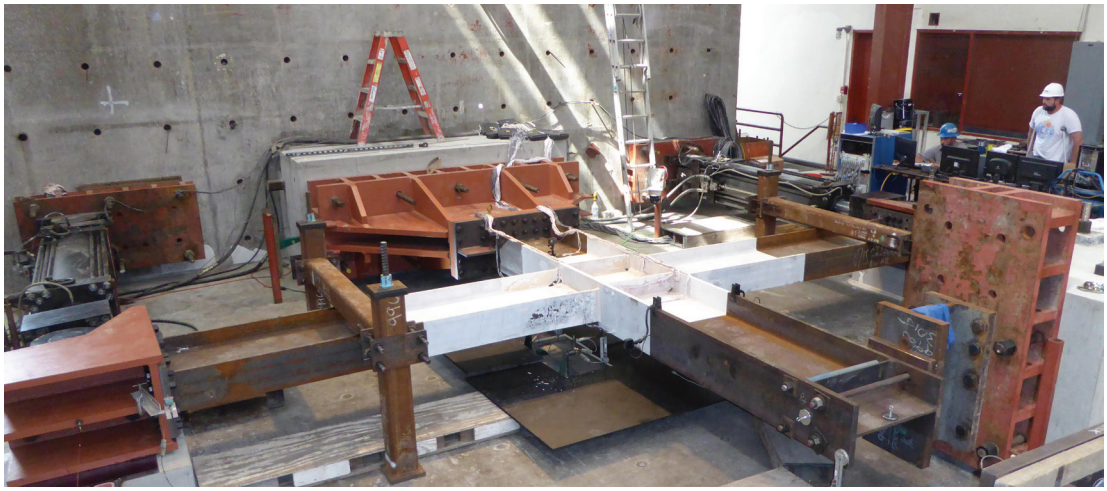

Fig. 2. Interior moment connection test setup.

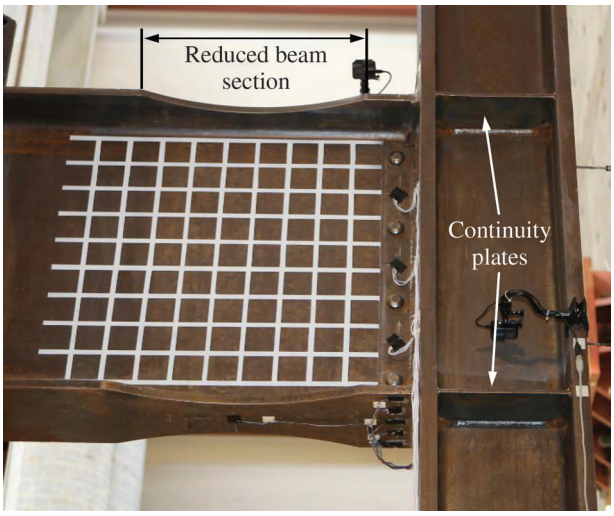

(a) Specimen C5 before testing

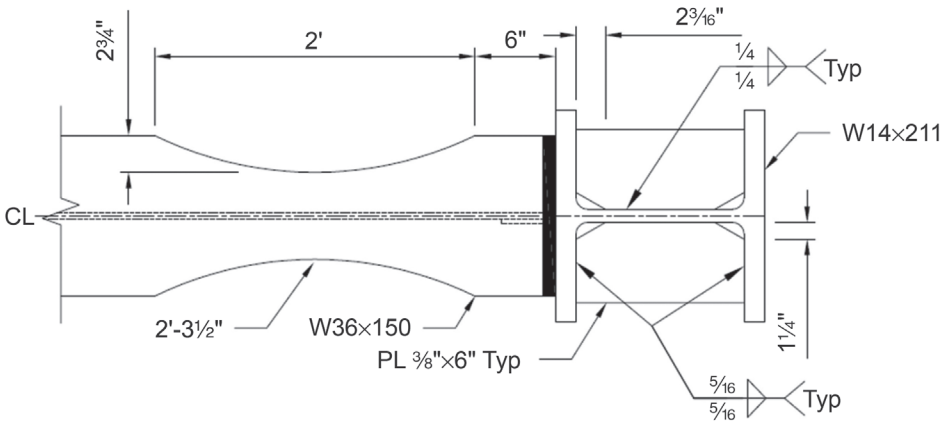

(b) RBS and continuity plate weld details

Fig. 3. One-sided RBS connections.

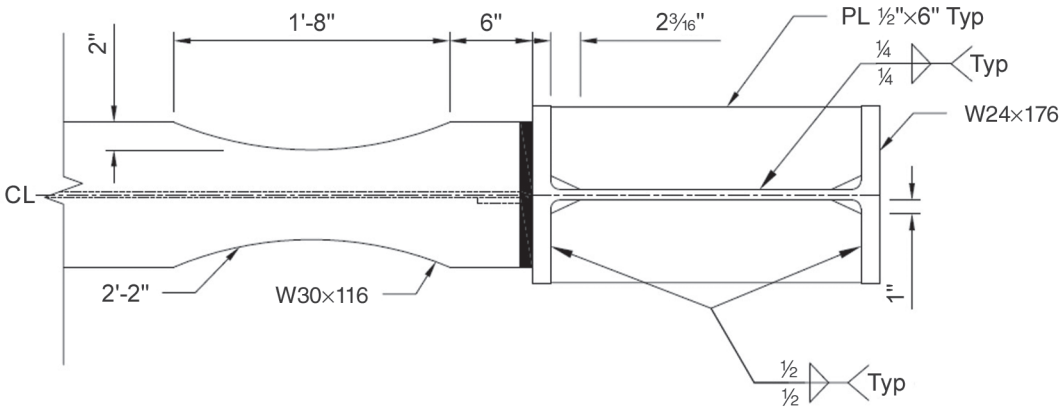

Fig. 4. Section through specimen C6 column showing continuity plates and RBS flange cuts.

Welded Unreinforced Flange–Welded Web (WUF-W) Specimen W2

Specimen W2 used a W33×141 beam and featured continuity and doubler plates, as shown in Figures 5 and 6. The continuity plates were intentionally overloaded to investigate any detrimental effects. The continuity plates satisfied the AISC *Seismic Provisions* requirement of a thickness of at least three-quarters of the beam flange thickness for interior connections. According to the plastic methodology, the continuity plates were undersized, with a demand-to-capacity ratio of 1.43. The continuity plate welds to the W27×217 column flanges were sized using the proposed $w = (¾)t_{cp}$ rule. A pair of ¾-in. doubler plates extended 6 in. above and below the beam flange elevations. Vertical partial-joint-penetration (PJP) groove welds connected the doubler plates to the columns.

Experimental Results

Specimens C5, C6, and W2 confirmed the proposed design methodology and exhibited satisfactory performance. The continuity plate-to-column flange welds showed no signs of distress for the 7 (of 10) specimens tested with a continuity plate in this research program. Despite specimen W2's intentionally undersized continuity plates, there was no continuity plate yielding and only minor panel-zone yielding in the doubler plates. The global load-displacement and moment-story drift response for specimen C5 are shown in Figure 7. Similar results were recorded for specimen C6. The column shear versus story drift response for specimen W2 is shown in Figure 8. All 10 specimens tested in this research satisfied the strength and story drift angle acceptance criteria of 0.04 rad (AISC, 2016a).

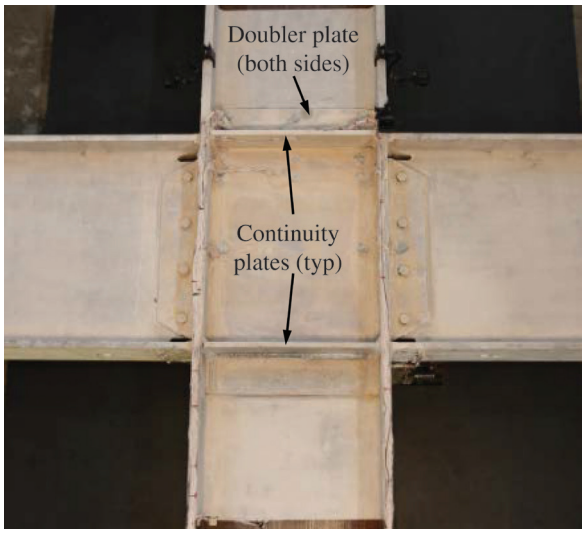

Fig. 5. Specimen W2 before testing.

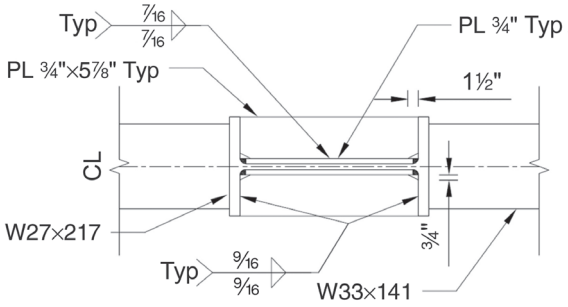

Fig. 6. Specimen W2 continuity and doubler plate details.

Specimen C5 exhibited ductile behavior and experienced significant inelastic demands from column kinking and local buckling in the beam web, beam flange, and continuity plate [Figure 9(a).] Beam web and flange local buckling within the reduced section were not observed until the 0.04-rad drift cycles. A bottom flange continuity plate also started to develop local buckling at 0.04-rad drift. By 0.05-rad drift, local buckling was observed in both flanges, as well as in a continuity plate on either side of the web at the top and bottom flanges. Column kinking was observed throughout the testing of the specimen. Ductile tearing of the beam top flange CJP groove weld was first observed in the second negative excursion of 0.03-rad drift. The specimen eventually failed by fracture of the beam top flange CJP groove weld after completing two cycles of 0.05-rad drift, as shown in Figure 9(b). Slight beam lateral-torsional buckling was also observed at the end of testing.

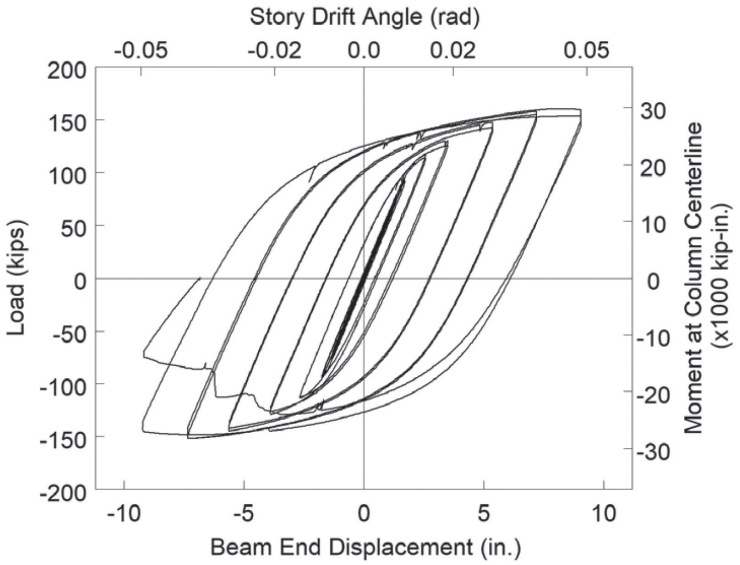

Fig. 7. Load-displacement and moment-story drift response for specimen C5.

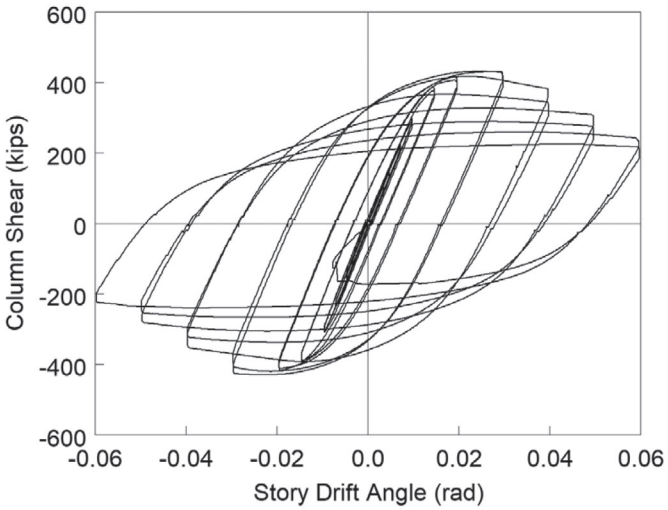

Fig. 8. Specimen W2 column shear versus story drift angle.

Specimen C6 also exhibited ductile behavior. Beam bottom flange yielding in the reduced section was observed during the 0.01-rad drift cycles. Panel-zone yielding commenced during the 0.015-rad cycles. Beam web buckling and beam flange local buckling as shown in Figure 10(a) did not start until the first cycle of 0.04-rad drift. Minor lateral-torsional buckling could also be observed. Minor ductile tearing of the beam top flange CJP groove weld began in the first negative excursion to 0.03-rad drift. In the 0.05-rad cycles, specimen C6 experienced a sudden fracture propagation at –0.037 rad, as shown in Figure 10(b), which led to complete fracture at –0.05-rad drift.

It should be noted that only a few RBS specimens failed at the beam flange-to-column CJP groove weld. Furthermore, ductile tearing preceded the eventual weld fractures. Specimen C6-G, galvanized but otherwise identical to specimen

(a) After testing *(b) Top-flange fracture*

Fig. 9. Specimen C5 testing results.

(a) After testing *(b) Fracture in top flange CJP groove weld during test*

Fig. 10. Specimen C6 testing results.

C6, did not fail at the weld but with a low-cycle fatigue fracture in the reduced beam flange. Based on the experimental and cyclic void growth model results, Reynolds (2020) attributed the likelihood of fracture to the "variability in weld surface topology (i.e., how sharp the reentrant corner is formed between the beam flange and column flange) and variability in weld notch toughness."

Specimen W2's response was initially governed by yielding of the flanges, which started during the 0.0075-rad drift cycles. Beam flange and web local bucking initiated at 0.03 rad. The second cycle at 0.03-rad drift was also the start of a weld fracture in the east beam top flange at the root of the CJP groove weld. The 0.05-rad drift cycles would see a weld tear on the top side of the west beam bottom flange CJP groove weld near the beveled fusion face of the CJP groove weld. A fracture was also observed in the east beam bottom flange CJP groove weld at 0.06-rad drift. These fractures would progress until the second cycle of 0.06-rad drift, when specimen W2 failed by fractures of the east top and west bottom beam flange CJP groove welds, as shown in Figures 11(a) and 11(b). Meanwhile, significant lateral-torsional buckling was observed initially at 0.04-rad drift and, together with flange and web local buckling, was quite severe by the end of the test, as shown in Figure 11(c).

FINITE-ELEMENT STUDIES

A computational parametric study was used to supplement the experimental investigation and verify the proposed methodology (Reynolds, 2020). The finite element analysis (FEA) was validated against the experiments. Parameters included column flange and continuity plate thickness.

The finite element model was validated through comparisons to the experimentally measured load-displacement response of the specimens; observed displacement patterns; and local estimates of accumulated equivalent plastic strain, PEEQ. The beams and columns were modeled as plate assemblies and meshed with shell elements using ABAQUS

(a) Fracture 1 at top flange

(b) Fracture 2 at bottom flange

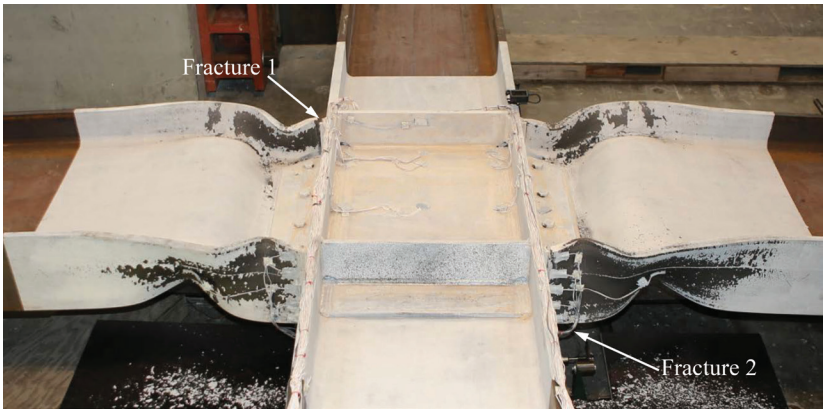

(c) End of test

Fig. 11. Specimen W2 fractures.

CAE (2014). The models did not include the flange-web fillets but did incorporate offsets to properly account for element thickness. The model geometry reflected the appropriate flange cuts in the reduced beam sections and the beam web cuts for the weld access holes. A mixed hardening model in ABAQUS was used for the steel; the mixed model is based on Lemaitre and Chaboche (1990). The cyclic hardening parameters were calibrated using measurements from 23 full-scale, deep-column tests conducted at UCSD (Chansuk et al., 2018). The NLGEOM option in ABAQUS within each explicit analysis step was used to capture geometric nonlinearity. Boundary conditions reflected the test setup and included lateral restraint of the beam at half the beam-depth away from the plastic hinge location. A comparison of the experimental and FEA results for specimen C5 illustrated in Figure 12 shows the ability of the FEA to capture the cyclic, global, load-drift response. The FEA is also able to capture behaviors such as the column kinking and continuity plate local buckling in specimen C5, as shown in Figure 13. Additional details of the model and validation can be found in Reynolds (2020).

Among the parameters investigated during the parametric study were the thickness and width-to-thickness ratio, b/t, of the continuity plate. Effects of normalized continuity plate thickness on continuity plate forces were explored, with comparisons to limit states such as WLY. Given the intentional continuity plate local buckling in specimen C5, the width-to-thickness ratio and instability of the continuity plate were also examined. At high ratios, plate instability resulted in significant bending stresses of the continuity plate. Figure 13 shows local buckling in the FEA of specimen C5 with continuity plate $b/t = 15.7$. Note that $b/t = 16.0$ in the experiment. For plates with a width-to-thickness ratio of 13.5, selected to correspond to $0.56\sqrt{E/R_yF_y}$, local buckling did not occur. The parametric study results suggested that this width-to-thickness limit is applicable to exterior and interior RBS and WUF-W connections.

PROPOSED REVISIONS IN THE AISC SEISMIC PROVISIONS

The experimental program and finite element parametric study have provided a basis for proposed changes to the AISC *Seismic Provisions*. Specifically, a limiting width-to-thickness ratio for continuity plates and the use of fillet welds in lieu of CJP groove welds are recommended. In the test program, the continuity plates with width-to-thickness ratio of 12 did not develop any local instabilities. The computational parametric study confirmed the recommended width-to-thickness limit of $0.56\sqrt{E/R_yF_y}$ for continuity plates. Meanwhile, no failures were observed in the capacity-designed fillet welds connecting the continuity plates to the columns.

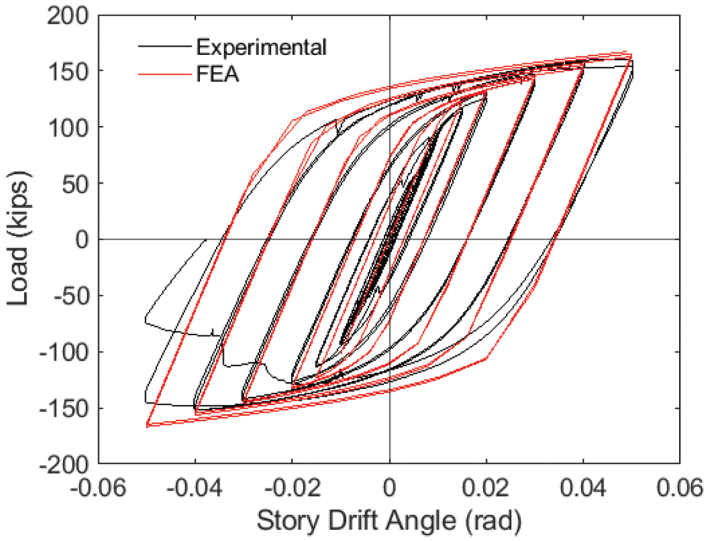

Fig. 12. Comparison of FEA to experimental load-drift response for specimen C5.

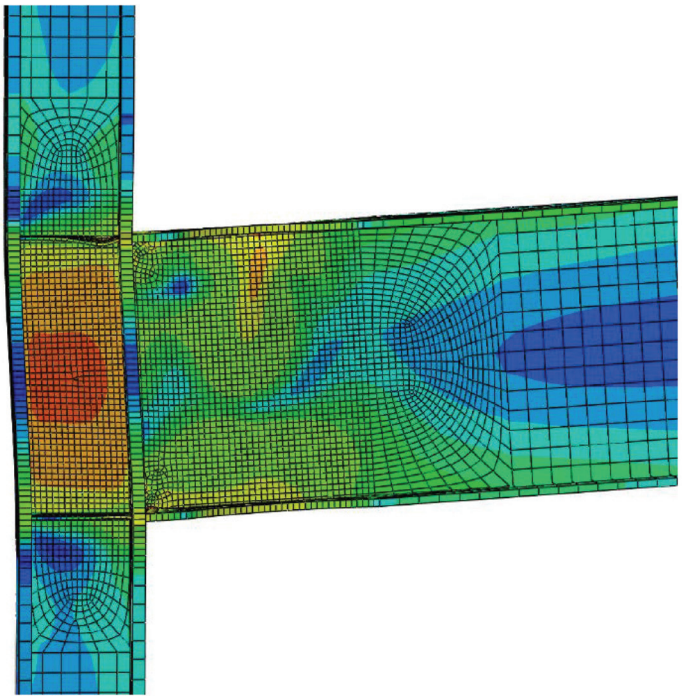

(a) Column kinking in FEA

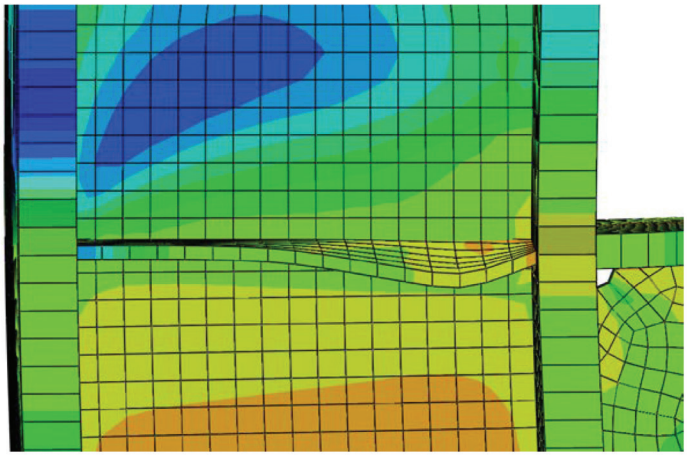

(b) Continuity plate buckling in FEA

(c) Continuity plate buckling in experiment

Fig. 13. Specimen C5 column kinking and continuity plate buckling.

SUMMARY

Recent advances in continuity plate design for special and intermediate moment frames have been highlighted. The comprehensive experimental and computational study by Dr. Mathew Reynolds and Dr. Chia-Ming Uang has supported the development of improved design procedures for continuity plates and their welds. A more efficient plastic design methodology for continuity plates includes procedures for fillet welds instead of CJP groove welds for connecting the continuity plates to the column flanges. Important outcomes of the research include a new continuity plate width-to-thickness limit and a capacity-design rule for sizing the fillet welds. Both provisions have been proposed for the 2022 version of the AISC *Seismic Provisions*.

This article has provided a sampling of the research, a larger effort that also included investigation into provisions for doubler plates. Publications that are in preparation include a detailed experimental results paper and a paper focusing on the parametric FEA results. The experimental results paper will contain design details and results for all test specimens, as well as additional recommendations for continuity and doubler plate design. The finite element analysis paper will provide extensive discussion of the parametric study results that support the proposed design methodology. The experimental results and the associated FEA are also available in Reynolds and Uang (2019) and Reynolds (2020).

ACKNOWLEDGMENTS

Thank you to Dr. Chia-Ming Uang and Dr. Mathew Reynolds for their editorial and other contributions to this article. Special thanks to Dr. Reynolds for all of the materials, coordination, edits, and additional feedback. The research was sponsored by the American Institute of Steel Construction (AISC); Mr. Tom Schlafly and Dr. Devin Huber served as project managers. The Herrick Corporation donated the fabrication of the specimens, and the Smith-Emery Company donated inspection services. The researchers also would like to acknowledge their Advisory Committee: Tim Fraser, Tom Kuznik, Kim Roddis, Subhash Goel, and Brian Volpe, with James Malley serving as the chair. Any findings or recommendations are those of the researchers and do not necessarily reflect the views of the sponsors.

REFERENCES

ABAQUS (2014), *Abaqus Standard User's Manual*, Version 6.14, Dassault Systemes Simulia Corp.

AISC (2016a), *Seismic Provisions for Structural Steel Buildings*, ANSI/AISC 341-16, American Institute of Steel Construction, Chicago, Ill.

AISC (2016b), *Specification for Structural Steel Buildings,* ANSI/AISC 360-16, American Institute of Steel Construction, Chicago, Ill.

AISC (2020), *Prequalified Connections for Special and Intermediate Steel Moment Frames for Seismic Applications*, including Supplements No. 1 and No. 2, ANSI/AISC 358s2-20, Chicago, Ill.

AWS (2016), *Structural Welding Code—Seismic Supplement*, AWS D1.8/D1.8M:2016, American Welding Society, Miami, Fla.

Chansuk, P., Ozkula, G., and Uang, C.-M. (2018), "Seismic Behavior and Design of Deep, Slender Wide-Flange Structural Steel Beam-Columns: Phase 2 Testing," Rep. No. SSRP-18/02, University of California San Diego, San Diego, Calif.

Dowswell, B. (2015), "Plastic Strength of Connection Elements," *Engineering Journal*, AISC, Vol. 52, No. 1, pp. 47–66.

Lemaitre, J. and Chaboche, J.-L. (1990), "Mechanics of Solid Materials," Cambridge International Press.

Mashayekh, A. and Uang, C.-M. (2018), "Experimental Evaluation of a Procedure for SMF Continuity Plate and Weld Design," *Engineering Journal*, AISC, Vol. 55, No. 2, pp. 109–122.

Reynolds, M. (2020), "Alternative Weld Details and Design for Continuity Plates and Doubler Plates for Applications in Special Moment Frames," University of California, San Diego, La Jolla, Calif. ProQuest ID: Reynolds_ucsd_0033D_19175. Merritt ID: ark:/13030/m5xh4zg9. Retrieved from https://escholarship.org/uc/item/32t492xx.

Reynolds, M. and Uang, C.-M. (2019), "Alternative Weld Details and Design for Continuity Plates and Doubler Plates for Applications in Special and Intermediate Moment Frames," Report SSRP-19/03, November, University of California, San Diego, La Jolla, Calif.

Tran, T.T., Hasset, P.M., and Uang, C.-M. (2013), "A Flexibility-Based Formulation for the Design of Continuity Plates in Steel Special Moment Frames," *Engineering Journal*, AISC, Vol. 50, No. 3, pp. 181–200.